Analysis of urban thermal environments using satellite data and urban microclimate modeling

Georgiana GRIGORAS*[,1], Bogdan URITESCU[1]

*Corresponding author
[1]INCAS – National Institute for Aerospace Research "Elie Carafoli",
B-dul Iuliu Maniu 220, Bucharest 061126, Romania,
grigoras.georgiana@incas.ro

DOI: 10.13111/2066-8201.2024.16.3.4

Received: 26 July 2024/ Accepted: 19 August 2024/ Published: September 2024

Abstract: *The aim of this paper is to analyze the influence of two types of urban morphology existing in the area of Bucharest on the local microclimate, using Landsat satellite data, GIS techniques and numerical modelling. The two types of urban design analyzed are differentiated by the period in which they were constructed, one being built in the communist era and the other in the current period. The phases of the study are: i) geospatial analysis of urban morphology focusing on the urban design features of each period; ii) spatial analysis of the land surface temperature in relation with urban geometry, using Landsat 9 satellite images; iii) simulation of microclimate using ENVI-met software to highlight the local thermal environment. Satellite data analysis highlighted higher values for the land surface temperature in neighborhoods built in the current period compared to the areas built in the communist era. The results of the simulation highlight the distinctions in the thermal environment between the two categories examined, lower values of air and surface temperatures for the neighborhoods built in the communist era.*

Key Words: *urban microclimate, remote sensing, numerical simulation, urban morphology*

1. INTRODUCTION

Globally, the movement of people from rural regions to urban centers has resulted in the growth of urban spaces. This urban development transforms green spaces, farmland, wetlands, and bodies of water into city landscapes [1]. Furthermore, rapid urban growth transforms the structural characteristics of the city, resulting in an expanded built-up environment and increasing the building density. This shift alters the proportion of average heights of building relative to the distance between them (width of the roads), contributing to the formation of street canyons and creating thermal variations throughout the urban landscape [2-7]. The fast urbanization process characterized by solar radiation being absorbed, heat being stored in built-up surfaces, roughness being increased and having a decreased evaporation, is considered to be the major factor causing the Urban Heat Island phenomenon (UHI). The UHI is characterized by higher values of air and surface temperatures in the urban area compared to the surrounding rural areas due to human activities [8-10].

As a result of the heat island effect, summer temperatures in urban areas are becoming increasingly unbearable, leading residents to rely more heavily on air conditioning. This dependence, in turn, significantly increases the level of anthropogenic heat released, creating a detrimental cycle. Therefore, thoughtfully designed cities can greatly enhance the urban thermal environment and mitigate the urban heat island effect [11-12].

The present paper represents a continuation of the studies carried out by the authors on the influence of urban morphology on the urban microclimate and the analysis of the urban heat island, presented in a series of publications [13-17]. This study aims to highlight the thermal conditions in urban areas defined by two distinct types of urban morphology that emerged from different approaches to urban planning. These two urban planning strategies are distinguished by their construction periods: one from the communist era (referring to 1968-1989 period) and the second which we call "the current period" (between 2010 and 2024). The impacts of these two urban development styles are examined through spatial analysis of land surface temperatures obtained from Landsat 9 satellite data, and through the simulation of surface and air temperatures using the urban microclimate model, ENVI-met [18].

2. DATA AND METHODS

2.1 The analyzed areas

To emphasize the two urban morphology types, the one from the communist period and the other from the current period, the buildings and the green spaces around them were vectorized from different areas of Bucharest, using the most recent satellite images from Google Earth, and the web portal of Green Cadastre of the Bucharest Municipality. The analyzed neighborhoods are presented in Figure 1. To accurately define the two periods, Google Earth historical imagery was used.

2.2 Obtaining LST

The satellite image was selected from the hottest period of 2024, being one of the few pictures with clear sky conditions available for that period. The image was taken at 12:02 local time (when the satellite pass across the analyzed area). Landsat 9 was used to calculate the LST for 09.07.2024 [19-20]. First, the digital numbers (DN) were converted to top of the atmospheric radiance value (TOA);

$$L_\lambda = M_L \times Q_{CAL} + \nabla_L \tag{1}$$

where: M_L is the radiance multiplicative scaling factor, Q_{CAL} corresponds to band 10 and ∇_L is the radiance additive scaling factor.

After that, the effective at satellite temperature (T_B) was computed as follows:

$$T_B = K_2/[\ln\left(\left(\frac{K_1}{L_\lambda}\right) + 1\right)] \tag{2}$$

where K_1 and K_2 are the first and second calibration constant for the thermal bands.

Finally, LST was retrieved after converting the at satellite brightness temperature (K) to surface temperature:

$$T_S = [\frac{T_B}{1 + \left(\frac{\lambda T_B}{\rho}\right) ln\epsilon}] - 273.15 \tag{3}$$

where: T_s is the surface temperature (°C), λ is the wavelength of radiance (11.5) and ε is the spectral emissivity.

$$\rho = h \times (c/\sigma) \quad (4)$$

where: h = Planck's constant (6.626 *10 $^{-34}$ Js), c =velocity of light and σ = Boltzmann constant.

$$\varepsilon = 0.02644Pv + 0.96356 \quad (5)$$

where: P_v = fractional vegetation cover can be obtained from:

$$Pv = [(NDVI - NDVImin)/(NDVImax - NDVImin)]^2 \quad (6)$$

where *NDVI* is the normalized difference vegetation index and is obtained from:

$$NDVI = (Near\ InfraRed\ band - Red\ band)/(Near\ InfraRed\ band + Red\ band) \quad (7)$$

2.3 ENVI-met numerical simulation

The ENVI-met model was used to simulate the urban microclimate for the selected areas [21-22]. ENVI-met is a sophisticated three-dimensional microclimate simulation model, based on the principles of fluid dynamics and thermodynamics, aiming to replicate the complex interactions between surface vegetation and air within urban settings. Numerical simulations were made for the day of 09.07.2024, for which the Landsat satellite image was also chosen.

The meteorological data used was recorded at the Filaret meteorological station (National Meteorological Administration). For the ENVI-met simulations, the following meteorological parameters have been defined: air temperature, wind speed and wind direction. Implicit values of ENVI-met were used for roughness length and specific humidity at the model top. The numerical stability of the model and the minimization of boundary effects, which may affect the output, have been secured by placing more nesting grids around the main model areas. The main modelling domain was: 150(x) * 150(y) * 40(z), with the 2 m step for each direction. In this paper, for the main field, results are presented only for the surface temperature and the air temperature at 2 m height, for the time when the Landsat 9 satellite passed.

3. RESULTS AND DISCUSSIONS

Two types of urban morphology, the one from the communist era (with enlarged green spaces) and the one from the current period (with larger built-up areas and decreased green areas), have been highlighted in this study, performing a geospatial analysis on Bucharest's four neighborhoods, located in two areas: east and south, each area containing one neighborhood built in the communist era and one in the current period. For a more accurate analysis, the digitized neighborhoods do not contain areas that include urban parks, commercial areas or administrative buildings.

The results of the analysis are displayed in graphical form in Figure 1 and in quantitative form (surface of analyzed area, surface and percentage of constructions in the analyzed area; surface and percentage of green spaces in the studied area) in Table1.

Additionally, a spatial analysis of the distribution of land surface temperatures obtained from satellite data was conducted (Figure 2). For each analyzed area there were obtained minimum values of LST (Ts MIN), maximum values (Ts MAX) and mean values (Ts MEAN) and the standard deviation was calculated (for the LST mean values presented in Table 1). The results presented in Table 1 show that the urbanization plan applied in the current period has the effect of reducing the green areas in favor of the built-up areas. Also, in correlation with the urban morphology types, it can be noticed that in the neighborhoods built in the current period, due to the increase of the surfaces occupied by buildings, the land surface temperature is more than two degrees higher.

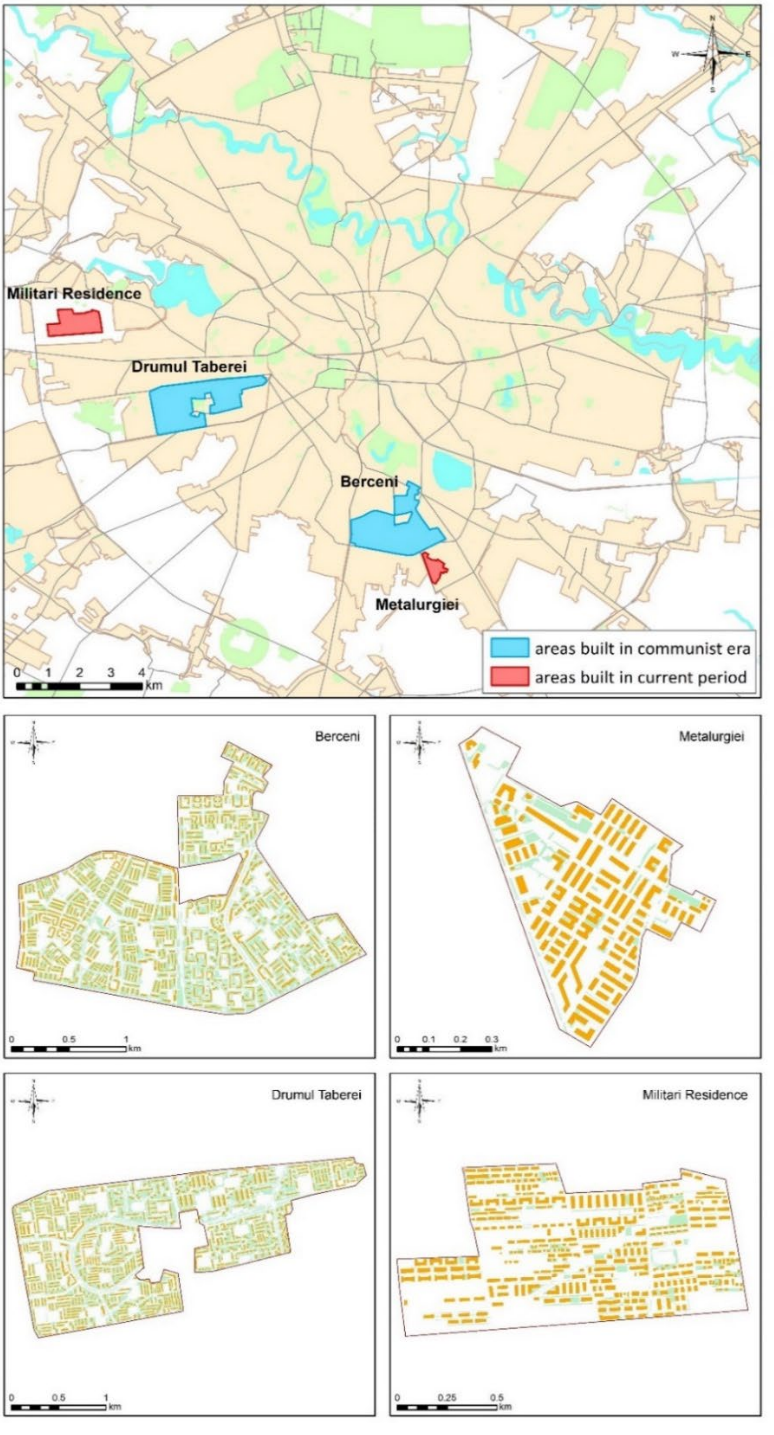

Fig. 1 Location of the analyzed neighborhoods in Bucharest and highlighting their urban morphology. Blue areas are neighborhoods built in the communist era; red areas are neighborhoods built in the current period. In each neighborhood, the green areas represent green spaces and the brown areas represent buildings

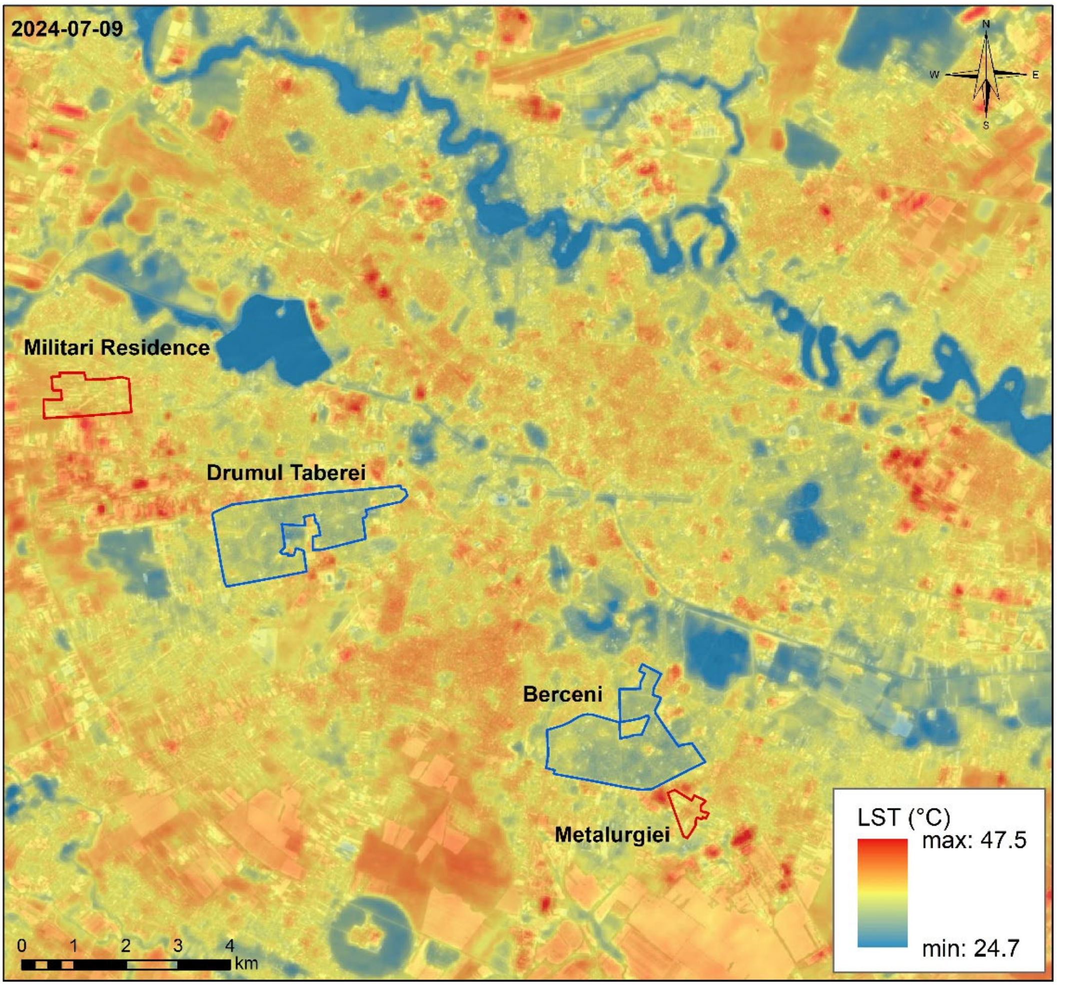

Fig. 2 Land surface temperatures derived from Landsat 9 image (09.07.2024)

Only LST values can be obtained from satellite images, therefore, for analyzing the local thermal environment, numerical simulations were carried out; land surface temperature and air temperature (another important component of UHI and urban microclimate) were simulated using the ENVI-met model for areas from the analyzed neighborhoods built in the communist era and in the current period.

Table 1. The spatial analysis results of the areas occupied by buildings and green spaces in the analyzed neighborhoods and the land surface temperatures corresponding to the analyzed areas

Neighborhood	Construction era	Surface area (km^2)	Buildings (km^2)	% Buildings from total area	Green spaces (km^2)	% Green spaces from total area	Ts MIN (°C)	Ts MAX (°C)	Ts MEAN (°C)	STD (°C)
Berceni	Communist	3.49	0.55	15.8	1.23	35.2	33.25	39.35	35.49	0.91
Drumul Taberei	Communist	3.61	0.57	15.8	1.25	34.6	33.94	39.39	35.98	0.86
Metalurgiei	Current	0.35	0.09	25.7	0.03	8.6	35.98	40.41	38.22	0.84
Militari Residence	Current	1.12	0.23	20.5	0.07	6.3	37.21	42.77	38.55	0.71

Fig. 3 Representation of areas for which urban microclimate simulations were conducted using the ENVI met model (top left – Berceni, top right - Metalurgiei, bottom left - Drumul Taberei and bottom right - Militari Residence)

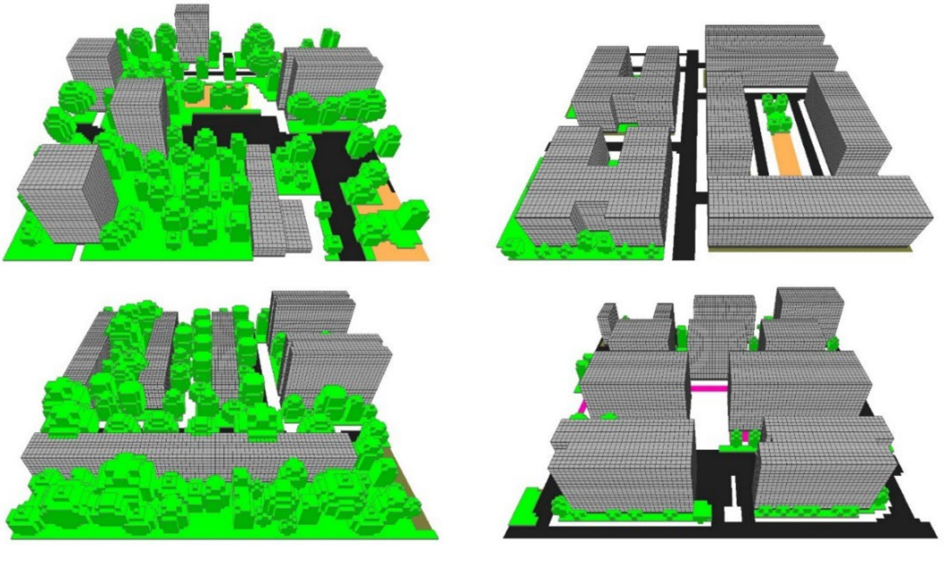

Fig. 4 Representation of the 3D models of the areas for which simulations of the urban microclimate were carried out using the ENVI-met model (top left – Berceni, top right - Metalurgiei, bottom left - Drumul Taberei and bottom right - Militari Residence)

For a better comparison, the analyzed areas from the neighborhoods built in the two periods, had the same surface and similar orientation of the buildings. The areas that have been compared from the neighborhoods are: Berceni with Metalurgiei and Drumul Taberei with Militari Residence (Figure 3).

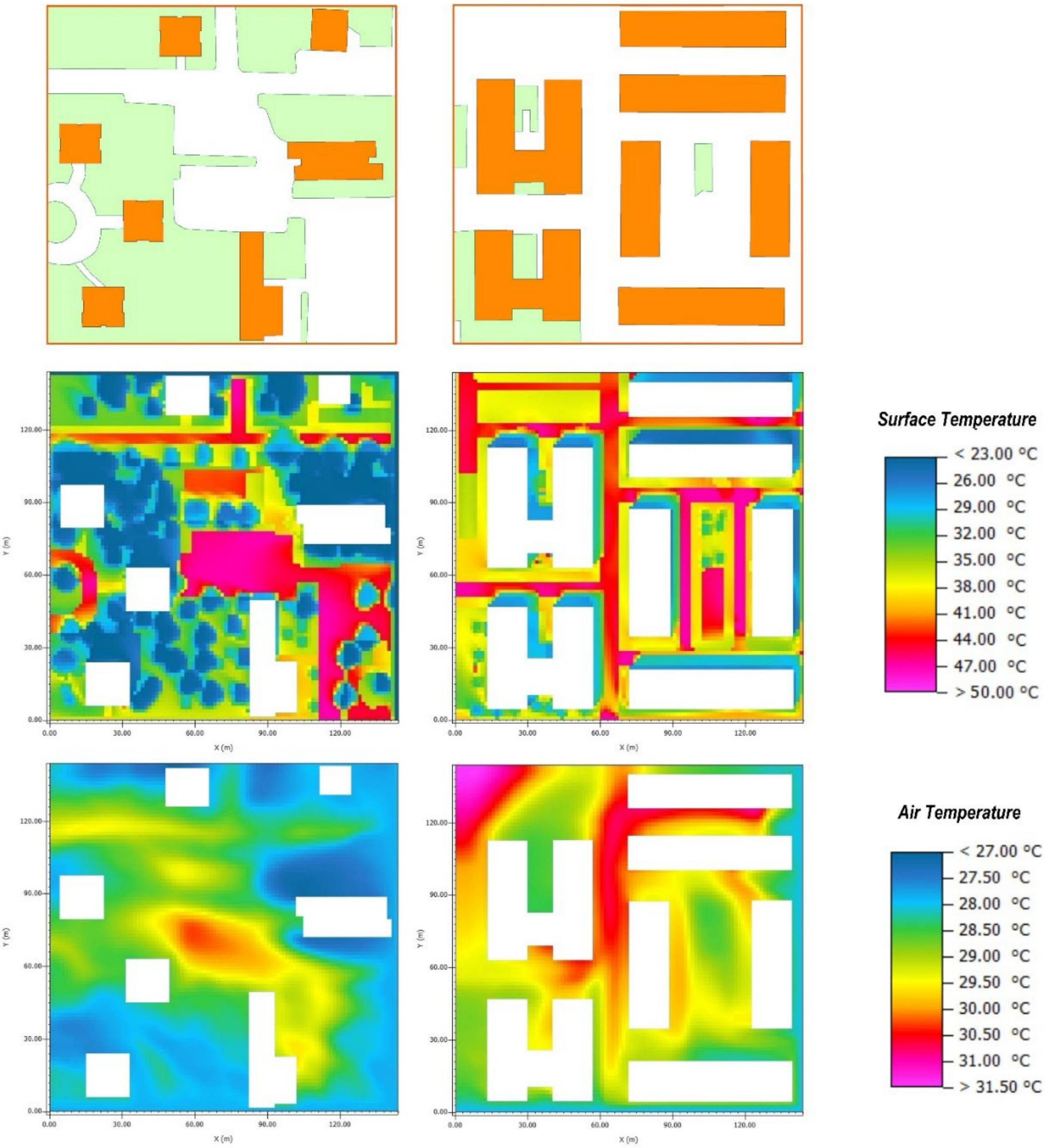

Fig. 5 Modeled land surface temperature and air temperature for 12:00, Berceni (left) and Metalurgiei (right), up - the digitized areas, middle - land surface temperature, down - air temperature at 2 m height

To simulate the local thermal environment, three-dimensional models for the analyzed areas were made, which constitute the input data in the urban microclimate simulation model, ENVI-met.

The 3D models of the four areas for which simulations were made are shown in Figure 4. Simulations of surface temperature and air temperature (at 2 m height) were performed for 12 o'clock.

For each analyzed area, the air temperatures (at 2 m height) and land surface temperatures resulted from simulations are represented in Figures 5 and 6.

These results are for the date and time when the Landsat 9 satellite passed over the studied areas.

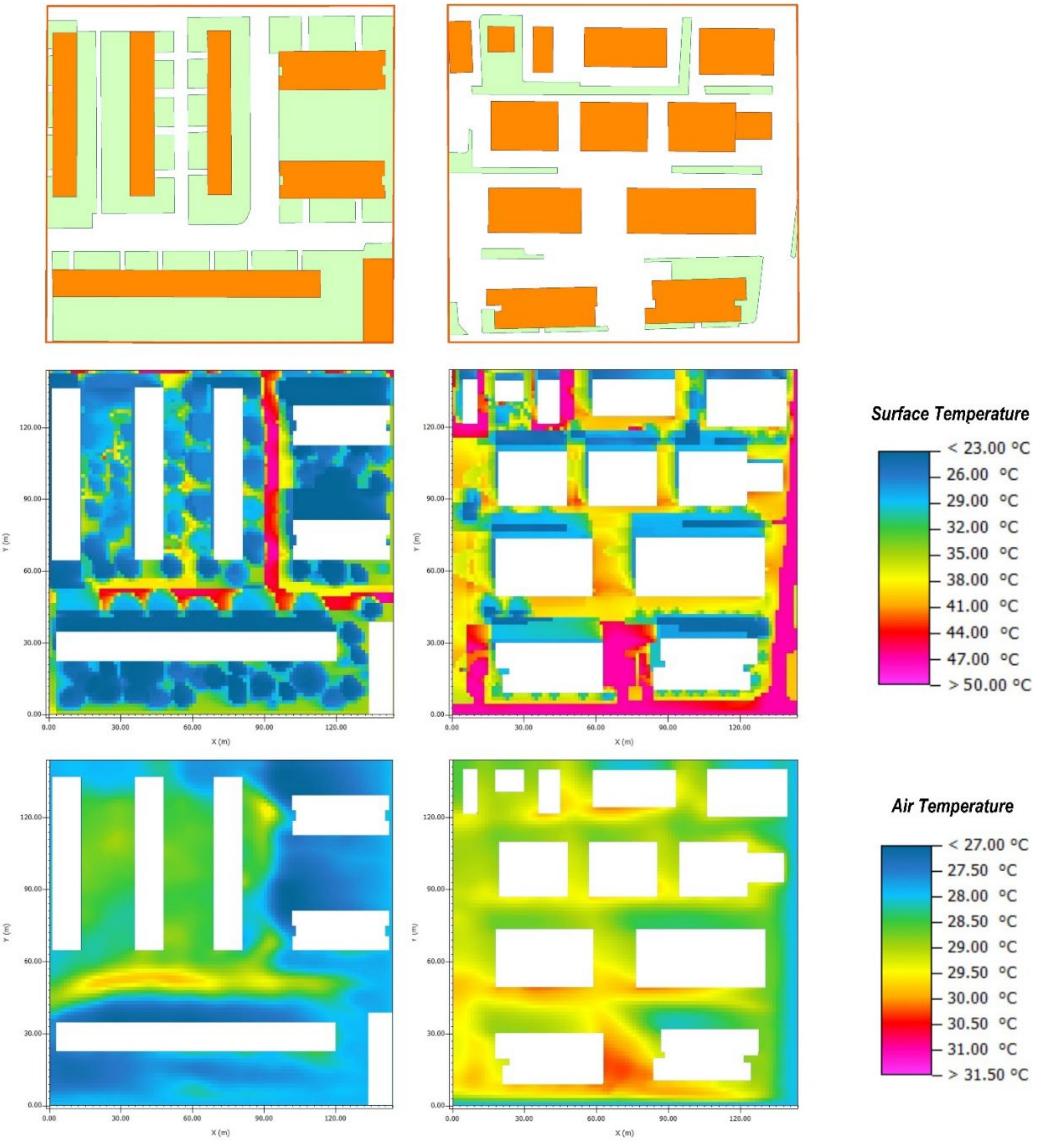

Fig. 6 Modeled land surface temperature and air temperature for 12:00, Drumul Taberei (left) and Militari Residence (right), up - the digitized areas, middle - land surface temperature, down - air temperature at 2 m height

The outcomes of the simulations highlight a variation in the temperature between 23 ℃ - 50 ℃ for LST and between 27 ℃ - 31.5 ℃ for air temperature.

The graphical representations of the simulation results indicate that regions constructed during the communist era exhibit extensive areas with low temperature values, whereas regions developed in the current period display high temperature values across larger areas.

The results of the surface temperature simulation (Figures 5 and 6) show differences in LST values between the two types of urban morphologies analyzed due to factors that vary from one area to another, such as: surfaces covered with concrete, asphalt surfaces, green spaces and shaded areas from tall buildings or dense vegetation like trees.

Examining images for the first urban morphology category, it turns out that areas with low temperatures values are generated by green surfaces, very widespread among buildings, that also contain a large number of trees. An additional characteristic is the low number of streets and concrete surfaces among the buildings which also contributes to lower LST values because vegetation has the property of reflecting the solar radiation in a larger quantity than surfaces made from concrete and asphalt). For the second urban morphology category, higher LST values can be observed due to the concrete and asphalt surfaces extended and the reduced green spaces. In the current period the areas occupied by green spaces compared to the built-up areas are smaller, there are more streets and alleys between buildings and the spaces occupied by parking spaces are larger compared to those of the communist era.

From the images representing air temperature values, a relation between the land surface temperature and the air temperature can be observed. There are small areas where the relation is not so visible because the air temperature is also influenced by other factors such as vertical surfaces (that can emit heat or create shadows) or due to trees which also produce shaded areas. For the images which represents the first urban morphology, high values of air temperatures can be observed on small areas that corresponds to streets, alleys and car parks that fell outside the shadow radius created by vertical bodies, or which are positioned in close proximity to structures.

Low air temperatures tend to be observed over large areas, particularly near buildings, primarily due to the abundance of green areas and the significant number of trees.

For the images that include areas built in the current period, high values of air temperatures can be observed due to hot areas (mostly streets and car parks) more numerous for these scenes, but also due to the small green areas and the lack of large trees presence.

4. CONCLUSIONS

The article analyzes two distinct types of urban morphology that have emerged due to different urbanization plans: one from the socialist era and the other from the current period.

The study highlights how these two forms of urban morphology influence the urban microclimates through geospatial analysis of land surface temperature distributions derived from Landsat 9 satellite data, along with simulations of land surface temperatures and air temperatures using the ENVI-met urban microclimate model.

The results indicate that the urban layout established during the socialist era features a greater proportion of green spaces, with an average ratio of 2.1 between green space coverage and built-up areas. In contrast, modern urban morphology places a greater emphasis on built-up areas, resulting in a different ratio between green spaces and built environments.

Urban morphology, which emerged in the current period, prioritize buildings construction, with an average ratio of green spaces to built-up areas being roughly 0.3.

Analysis of land surface temperatures, derived from Landsat 9 data, indicates that neighborhoods constructed in the current period experience average surface temperatures about 2-3 degree Celsius higher than those built during the socialist era.

Additionally, urban microclimate simulations conducted using ENVI-met reveal notable differences in the thermal conditions between these two urban morphology categories.

Neighborhoods established in the socialist era exhibit lower land surface temperatures and air temperatures when compared to those from the current period.

The results of this study reveal that the morphological characteristics have a strong effect on local temperatures highlighting the need for optimized urban plans that include urban heat island mitigation strategies such as building neighborhoods with a lower building density and more green spaces, which will increase outdoor thermal comfort.

ACKNOWLEDGEMENT

This work was supported by the contract nr. 36 N/12.01.2023 "PN - Advanced research to increase competitiveness and capacity for design, analysis and specific expertise in the aerospace field - AEROEXPERT 2023-2026", project code 23 17 08 02, with the title "Development of modeling and simulation capabilities of the Atmosphere-Earth system in synergy with airborne data", funded by Ministry of Research, Innovation and Digitalization.

REFERENCES

[1] S. K. Abd-Elmabod, M. A. Jiménez-González, A. Jordán, Z. Zhang, E. S. Mohamed, A. A. Hammam, A. A. El Baroudy, M. K. Abdel-Fattah, M. A. Abdelfattah, L. Jones, Past and future impacts of urbanization on land surface temperature in Greater Cairo over a 45 year period, *The Egyptian Journal of Remote Sensing and Space Science*, vol. **25**, no. 4, pp. 961-974, 2022.

[2] M. Unal Cilek, and A. Cilek, Analyses of land surface temperature (LST) variability among local climate zones (LCZs) comparing Landsat-8 and ENVI-met model data, *Sustainable Cities and Society*, vol. **69**, 102877, 2021.

[3] M. Wang, H. Xu, The impact of building height on urban thermal environment in summer: a case study of Chinese megacities, *PLoS ONE,* vol. **16**, no. 4, e0247786, 2021.

[4] J. Lin, S. Qiu, X. Tan, Y. Zhuang, Measuring the relationship between morphological spatial pattern of green space and urban heat island using machine learning methods, *Building and Environment*, vol. **228**, 109910, 2023.

[5] H. Zhang, C. Wang, H. Yang, Z. Ma, How do morphology factors affect urban heat island intensity? an approach of local climate zones in a fast-growing small city, Yangling, China, *Ecological Indicators*, vol. **161**, 111972, 2024.

[6] J. Zhang, Zhen Li, Dan Hu, Effects of urban morphology on thermal comfort at the micro-scale, *Sustainable Cities and Society*, vol. **86**, 104150, 2022.

[7] L. Zhou, B.Yuan, F. Hu, C.Wei, X. Dang, D. Sun, Understanding the effects of 2D/3D urban morphology on land surface temperature based on local climate zones, *Building and Environment*, vol. **208**, 108578, 2022.

[8] M. W. Shahfahad, Naikoo, A. R. Md. T. Islam, J. Mallick, A. Rahman, Land use/land cover change and its impact on surface urban heat island and urban thermal comfort in a metropolitan city, *Urban Climate*, vol. **41**, 101052, 2022.

[9] J. Yang, Y. Yang, D. Sun, C. Jin, X. Xiao, Influence of urban morphological characteristics on thermal environment, *Sustainable Cities and Society*, vol. **72**, 103045, 2021.

[10] Z. Wu, Z. Tong, M. Wang, Q. Long, Assessing the impact of urban morphological parameters on land surface temperature in the heat aggregation areas with spatial heterogeneity: A case study of Nanjing*, Building and Environment*, vol. **235**, 110232, 2023.

[11] B.-J. He, L. Ding, D. Prasad, Relationships among local-scale urban morphology, urban ventilation, urban heat island and outdoor thermal comfort under sea breeze influence*, Sustainable Cities and Society*, vol. **60**, 102289, 2020.

[12] S. W. Kim, and R. D. Brown, Urban heat island (UHI) intensity and magnitude estimations: A systematic literature review, *Science of The Total Environment*, vol. **779**, 146389, 2021.

[13] B. Uriţescu, N. Ionac, G. Grigoraş, The influences of land use on the urban heat island in Bucharest; "*Air and Water – Components of the Environment", Conference Proceedings*, Cluj-Napoca, Romania, pp. 259-265, 2017.

[14] G. Grigoraş, B. Uriţescu, Spatial hotspot analysis of bucharest's uhi using MODIS data, *Annals of Valahia University of Targoviste, Geographical series*, vol. **18**, no. 1, 2018.

[15] B. Urițescu, G. Grigoraș, N. Ionac, The Influence of Urban Morphology on the Urban Microclimate.2019, "*Air and Water – Components of the Environment", Conference Proceedings*, Cluj-Napoca, Romania, pp. 311-322, 2019.

[16] G. Grigoras, B. Uriţescu, Land Use/Land Cover changes dynamics and their effects on Surface Urban Heat Island in Bucharest, Romania", *International Journal of Applied Earth Observation and Geoinformation*, vol. **80**, pp. 115–126, 2019.

[17] B. Urițescu, G. Grigoraș, The Influence of Building Envelope on the Local Microclimate, "*Air and Water – Components of the Environment", Conference Proceedings*, Cluj-Napoca, Romania, pp. 140-153, 2022.

[18] * * * ENVI-met, http://www.envi-met.info/doku.php, 2024.

[19] * * * U.S. Geological Survey (USGS), https://www.usgs.gov/landsat-missions/landsat-9, 2024.

[20] S. Sannigrahi, S. Bhatt, S. Rahmat, B. Uniyal, S. Banerjee, S. Chakraborti, S. Jha, S. Lahiri, K. Santra, A. Bhatt, Analyzing the role of biophysical compositions in minimizing urban land surface temperature and urban heating, *Urban Climate*, vol. **24**, pp. 803-819, 2018.

[21] T. Haeri, N. Hassan, A. Ghaffarianhoseini, Evaluation of microclimate mitigation strategies in a heterogenous street canyon in Kuala Lumpur from outdoor thermal comfort perspective using Envi-met, *Urban Climate*, vol. **52**, 101719, 2023.

[22] Z. Liu, W. Cheng, C. Y. Jim, T. E. Morakinyo, Y. Shi, E. Ng, Heat mitigation benefits of urban green and blue infrastructures: A systematic review of modeling techniques, validation and scenario simulation in ENVI-met V4, *Building and Environment*, vol. **200**, 107939, 2021.